Experimental Validation of Mathematical Framework for Fast Switching Valves used in Digital Hydraulic Machines

Nørgård, Christian; Roemer, Daniel Beck; Bech, Michael Møller; Andersen, Torben O.

Published in:
Proceedings of the ASME/BATH 2015 Symposium on Fluid Power and Motion Control, FPMC 2015

DOI (link to publication from Publisher):
10.1115/FPMC2015-9612

Publication date:
2015

Document Version
Early version, also known as pre-print

Proceedings of FPMC'15
2015 ASME Fluid Power and Motion Control
October 12-14, 2015, Chicago, Illinois USA

DRAFT

FPMC2015-9612

EXPERIMENTAL VALIDATION OF MATHEMATICAL FRAMEWORK FOR FAST SWITCHING VALVES USED IN DIGITAL HYDRAULIC MACHINES

Christian Noergaard
Department of Energy Technology
Aalborg University
Aalborg East, 9220, Denmark
Email: chn@et.aau.dk

Daniel B. Roemer
Michael M. Bech
Torben O. Andersen
Department of Energy Technology
Aalborg University
Aalborg East, 9220, Denmark
Email: {dbr,mmb,toa}@et.aau.dk

ABSTRACT

A prototype of a fast switching valve designed for a digital hydraulic transmission has been manufactured and experimentally tested. The valve is an annular seat valve composed of a plunger connected with a direct electromagnetic moving coil actuator as the force producing element. Based on an elaborate optimization method the valve is designed to maximize the efficiency of a digital hydraulic motor targeted to a wind turbine transmission system. The optimisation method comprises a mathematical framework which predicts a valve switching time of approximately 1 ms with a peak actuator input power of 10 kW during switching (mean of approximately 250 W) and a pressure loss below 0.5 bar at 600 l/min. The main goal of this article is validate parts of the mathematical framework based on a series of experiments. Furthermore, this article aims to document the experience gained from the experimental work and to study and assess a moving coil actuators suitability for the application.

INTRODUCTION

Fluid power transmissions feature compact designs with high torque densities but traditionally also relatively low energy efficiencies, especially at part load. Recent advances in fluid power technology enable hydraulic transmissions to achieve higher efficiencies by use of digital hydraulic (DH) machines, also known as Digital Displacement® machines [1–3]. Digital hydraulic pumps and motors are a maturing technology, where progress have been made the last decades. Large scale DH machines suitable for wind turbines or wave energy transmission systems are being developed [4] and the very first large scale DH transmission systems are now being exploited commercially [5]. DH machines consist of a number of pistons and pressure chambers arranged around a crank shaft (or eccentric etc.) which each are connected to a low- and high pressure manifold through two independently electronically controlled seat valves. Figure 1 shows a hydraulic diagram of a single chamber and valves in a DH machine. The valves of each pressure chamber are controlled accordingly to the piston movement to either add or subtract oil from the high pressure manifold (pumping/motoring) or be disabled by keeping the low pressure valve (LPV) open for the entire piston cycle (idling). During idling operation, the pressure chamber is not pressurized which leads to lower energy losses. DH pumps/motors may potentially increase the efficiencies of fluid power transmissions as they are capable of maintaining high efficiencies, also when operating with relatively low displacements where traditional fluid power pumps/motors typically suffer from from low or mediocre efficiency [6].

In DH pumps and motors a number of pistons are arranged around and connected to a crankshaft. The displacement of the pump or motor is controlled in discrete steps by changing the states of each pressure chamber between either motoring or pumping and idling. Figure 2 shows an example of the valve sequence for a motoring and a pumping cycle of a single pressure chamber. A core element of DH machines is the use of leakage free seat valves and relatively weak actuators using only little

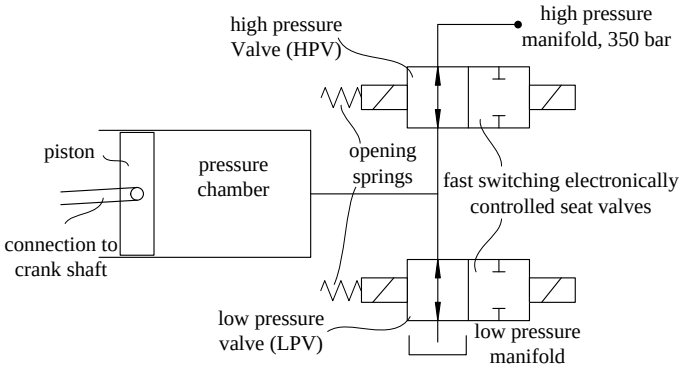

Figure 1. Hydraulic diagram of a single pressure chamber in a digital hydraulic fluid power pump/motor. Two fast electronically switched seat valves and a piston are connected to a pressure chamber. The operation mode (pumping, motoring, idling) is determined by the valve control sequence.

input power. The fast switching actuators are generally much weaker than the pressure forces acting to close the valves against their seats. However, by actuating the valves electrically at time instants synchronized to the piston movement the DH machine may be operated without needing to open nor close the valves against high pressure forces [7].

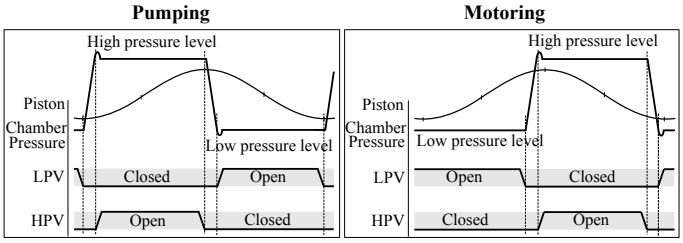

Figure 2. Example of motoring and pumping operation modes of DH machines. Pumping, motoring and idling are possible by changing the valve sequence.

The derived prototype valve design tested in this paper is an optimum with respect to switching time and flow coefficient ($\sqrt{\Delta p}/Q$) derived through an optimisation method proposed in [8]. Initial studies have shown that both the flow coefficient and the switching time influences the efficiency of DH machines significantly [2]. Today, no commercial large flow valves are available, which exhibits low enough switching time and flow coefficient for DH machines to constitute an attractive alternative to traditional drive train systems. The state of the art for fast switching large flow valves are prototype designs based on pilot actuated seat valves where a switching time of approximately 1.5 ms and a flow coefficient around 0.02 $\sqrt{\text{bar}} \cdot \text{min}/\text{l}$ [9, 10] has been demonstrated. The valve in focus is a seat valve featuring an electromagnetic moving coil actuator. The results presented in this paper shows that the valve design may advance the state of the art of publicly known suitable valves, as a switching time of approximately 1.2 ms is documented and a flow coefficient of 0.001 $\sqrt{\text{bar}} \cdot \text{min}/\text{l}$ is predicted based on the mathematical framework. This facilitates improvement of the efficiency of DH machines. Figure 3 shows pictures of the valve prototype.

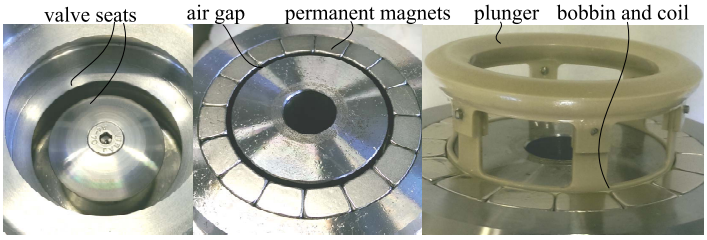

Figure 3. The valve prototype.

Initially the paper reviews the DH technology and a reference DH motor design the valve prototype is designed for. Then, focus is turned towards the mathematical framework which is validated through the tests that have been performed on the valve. Finally the measurements are compared to simulation results to assess the time dependent performance of the valve and to verify the mathematical framework.

BACKGROUND AND VALVE APPLICATION

The Digital Displacement technology was invented by a research team at the University of Edinburgh, who later founded the company Artemis Intelligent Power Ltd (AIP). AIP filed for patent of their first DH pump in 1989 [11], and followed with the DH motor in 1990 [12]. Today, DH technology is commercially used, but only in applications with lower power levels than needed in the wind turbines e.g. in off road vehicles, trains etc. [13]. In 2011 Mitsubishi Heavy Industries announced plans for testing a wind turbine in the 7 MW class based on the Artemis technology, but detailed information is still not published [14]. Although no detailed information is available regarding valve performance or design specifications, the valves installed in the machine appear to be direct actuated seat valves, with a variable reluctance (solenoid) actuator as the force producing element, based on graphics included in the patent applications [15–17].

Prior to optimisation of the design, knowledge of the valve application is needed. Therefore, a preliminary design of a DH motor have been made, see Fig. 4. The preliminary design consists of a number of identical slices (wedding cake assembly). In principle, the rated motor power may be changed by changing the number of slices in the motor. The high pressure manifold distributes the high pressure oil to each pressure chamber which drives the piston and in turn drives the motor shaft through an eccentric. A sectional view of the reference design, including

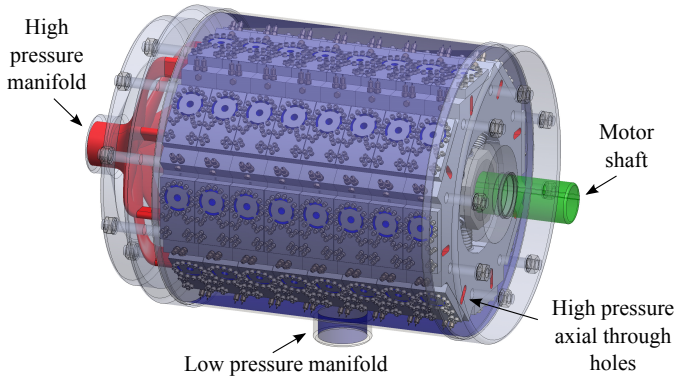

Figure 4. Prelimenary hydraulic dh motor with 64 pressure chambers.

details of a single pressure chamber, is shown in Fig. 5. Low pressure loss for the LPV is prioritized above pressure loss of the HPV to improve part load efficiency (due to flow through LPV during idling) therefore the LPV is positioned directly above the piston. The valves are manipulated by electromagnetic moving coil actuators which appear to be one of the fundamental differences between the reference design and state of the art DH machines using variable reluctance actuators. Initial studies [18] indicates that moving coil actuators have superior transient response compared to variable reluctance actuators. The main specifications of the reference DH motor design is shown in Tab. 1.

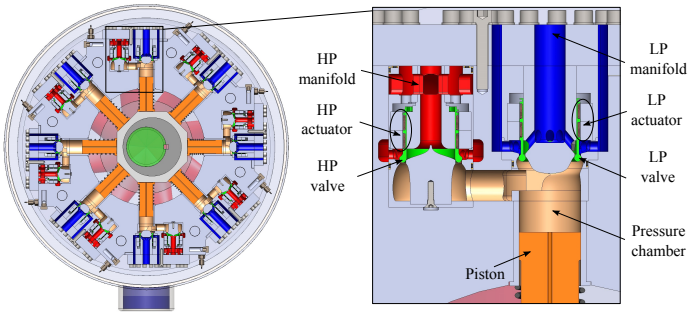

Figure 5. Sectional view of motor slice with a zoom of a single pressure chamber with HP and LP valve and actuator.

Table 1. Main specs. for ref. DH motor.

Rotation speed	1500 rpm
Cylinders	64
Total power	3-7 MW
Overall size	Ø1.2x1.5 m
Manifold pres. high/low	350/5 bar
Displacement total/cyl	9024/141 cc

MATHEMATICAL FRAMEWORK

The prototype is a design optimum derived based on a mathematical framework developed through a research project [1]. An elaborate optimisation method for DH motors were presented in [8] where several sub domains are optimized based on a chosen valve topology. This involves a mathematical framework, including transient Computational Fluid Dynamics (CFD) models, heat transfer modelling, structural Finite Element Analysis (FEA) and transient electromagnetic FEA [1]. The valve prototype installed in the current experimental setup allows us to verify the transient performance of the moving coil actuator when closing the LPV. The transient performance is an important part of the mathematical framework as the valve switching time have been shown to have significant influence on the efficiency of DH machines [1]. Modelling of the valve closing specifically involves transient CFD analysis to describe the fluid forces that oppose the valve plunger when closing besides transient electromagnetic FEA to simulate the time dependent performance of the moving coil actuator. Details of these models are given in the following sections.

MODELLING OF FLUID FORCES

To derive an optimal actuator design for the application the actuator load must be determined. Therefore, transient CFD analysis have been utilized to determine the fluid forces (including acceleration of virtual mass) that oppose the plunger when closing. Based on the transient CFD analysis a lumped parameter model is derived which is simulated simultaneously with the transient electromagnetic FEA actuator model of the moving coil actuator.

The CFD simulations are carried out in Ansys Fluent where dynamic re-meshing and layering zones are used to incorporate the plunger movement in the simulation (see Fig. 6, left). The fluid forces that oppose the plunger movement when closing are simulated with the plunger considered to be submerged in stationary oil. This neglects the flow related fluid forces which is a conservative assumption with respect to valve closing time as the flow induced fluid forces contributes to closing of the valve. Developing an accurate and fast executable model (lumped parameter) that accounts for the flow induced fluid forces is a time consuming task as it involves a number of transient CFD simulations. Also, the flow related fluid forces are not suspected to be significant since the valve closings are conducted when the piston velocity and hence the flow rates are low (see Fig. 2). The lumped parameter description of the fluid forces have been obtained using 2D transient CFD simulations in [19]:

$$F_f = m_v\ddot{y}_p + \left(B + k_1 + k_2 e^{-\frac{l_s - y_p}{k_3}} + k_4 e^{-\frac{l_s - y_p}{k_5}}\right)\dot{y}_p + D\dot{y}_p^2 \quad (1)$$

where y_p is the plunger position, m_v denotes the virtual mass

added due to acceleration of the surrounding fluid, B the viscous shearing coefficient, D the drag coefficient and $k_1..k_5$ are additional friction coefficients. The viscous shearing friction coefficient B is not part of the transient CFD simulations hence it is separately calculated from the shearing friction present in the inside of the bobbin region using the expression:

$$B = \nu\rho\left(\frac{A_{b,inside}}{g_1} + \frac{A_{b,outside}}{g_2}\right) \quad (2)$$

where ν is the kinematic oil viscosity, ρ the oil density, $A_{b,inside}$ and $A_{b,outside}$ the shearing area of the inside and outside of the bobbin respectively, g_1 and g_2 the inside and outside shearing layer thickness respectively (see Fig. 7). It is of interest to validate the fluid force model as it predicts the fluid forces to influence the closing of the valve significantly. A simulation of the transient CFD and the lumped parameter model is shown in Fig. 6 with a constant actuator force of 500 N. The acceleration shows that the plunger is slowed down considerably as the plunger comes near to the valve seat due to the increase in opposing fluid forces. Table 2 gives the fluid force coefficient values for the optimum design.

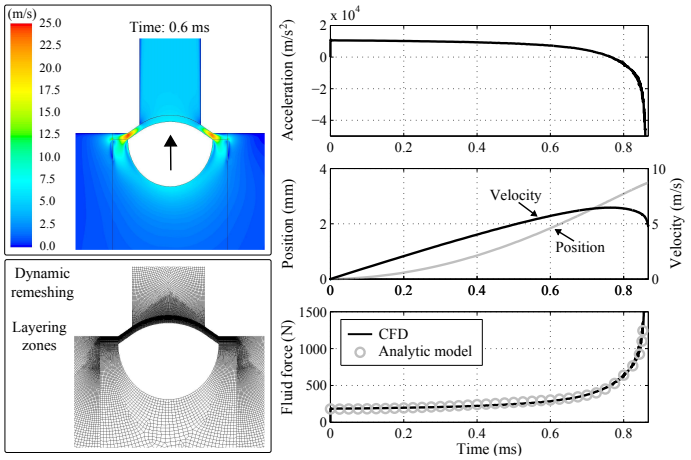

Figure 6. Simulation results for transient CFD and lumped parameter model when applying a constant actuator force of 500 N. Transient states are shown with a color plot of the flow velocity and the mesh used in the model.

Table 2. Fluid force coefficients for optimum valve design (at 1 bar).

Virtual mass m_v, B	17 g, 2.48 Ns/m
ν, ρ, (g_1, g_2)	$46{\cdot}10^{-6}$ m^2/s, 870 kg/m^3, (0.1, 0.25)mm
(k_1, k_2, k_3)	(0.002, 225, $3.952{\cdot}10^{-4}$)Ns/m
(k_4, k_5), D	(1968,$2.96{\cdot}10^{-5}$)Ns/m, 4.93 Ns^2/m^2

ACTUATOR MODEL

To simulate the time dependent response of the moving coil valve actuator a transient electromagnetic FEA coupled with the lumped parameter model that describes the fluid forces is utilized. This enables us to validate both the actuator and fluid force model by comparing simulations with measurements (see the results section). The actuator geometry of the prototype is primarily rotation-symmetric, hence the problem is modelled as a two dimensional problem to limit the computational burden. Figure 7 show how the actuator prototype is parametrized when using the transient electromagnetic FEA to find the optimum moving coil actuator for the valve application. Modelling of the electro magnetics is done by solving the magnetic vector diffusion equation with appropriate boundary conditions for the domain shown in Fig. 5 (including a surrounding air domain not shown in the figure). The magnetic vector diffusion equation is expressed as [20]:

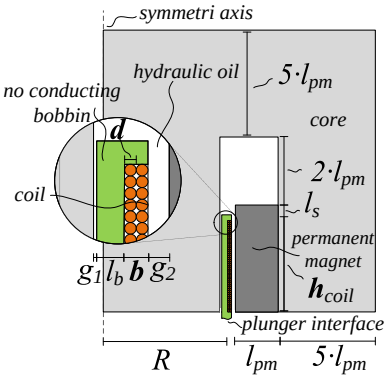

Par.	[mm]
$\boldsymbol{d}$	0.02
$\boldsymbol{b}$	0.4
$\boldsymbol{h}_{coil}$	20
g_1	0.1
l_b	1
g_2	0.25
R	30
l_{pm}	10
l_s	3.5

Figure 7. Rotation-symmetric representation of the moving coil actuator used in the transient FEA. The bold face parameters in the figure and table are the design variables in the optimisation scheme .

$$\sigma\frac{\delta \mathbf{A}}{\delta t} + \nabla \times \mathbf{H} - \sigma \mathbf{v} \times \mathbf{B} = \mathbf{J}_e \quad (3)$$
$$\mathbf{H} = \mathbf{f}(\mathbf{B}) \quad \text{and} \quad \mathbf{B} = \nabla \times \mathbf{A}$$

where σ is the material conductivity, $\mathbf{A}$ the magnetic vector potential, $\mathbf{H}$ the magnetic field strength, $\mathbf{v}$ the velocity of the conducting material, $\mathbf{B}$ the magnetic flux density and $\mathbf{J}_e$ the externally generated current density. The external current density is solved using co-simulation of an external circuit coupled to the field solution. Eqn. 3 is solved with $\mathbf{A}$ as unknown using the software package COMSOL Multiphysics 5.0 AC/DC module scripted through Matlab. To solve Eqn. 3 knowledge of materials properties are needed for all domains. In particular, the initial magnetization curve (BH-curve) and the electrical conductivity σ must be known for all materials of the domain shown in Fig.

Table 3. Magnetic and electrical properties.

	BH-relation [A/m,T]	Conductivity [S/m]
Copper (@ 100°C)	$\mu_r = 1.0$	$4.55{\cdot}10^7$
Magnet (NeFeB 35MGOe)	$\mu_r = 1.045$ $H_c = 9.15 \cdot 10^5$	0 (shell magnets)
Steel	Selected points:*(H,B)*= {(632,1.0), (61k,2.0), (318k,2.4)}	$6.29 \cdot 10^6$

7. The magnet strength and the steel path magnetization curve have been determined through experiments to improve the accuracy of the actuator model [21]. The magnet strength was determined by measuring the flux density around a magnet piece surrounded by air with a gauss meter. The electrical conductivity of the permanent magnets is approximated as zero since shell magnets are used in the prototype design. The used core material is low carbon construction steel where the magnetization curve is not specified. The magnetization curve have also been determined experimentally to increase the model accuracy. A toroid with the core material have been fabricated and used to experimentally measure the magnetization curve [21]. A typical value for the electrical conductivity of the core steel is used in the FEA. Material properties used in the model are summarized in Tab. 3. An example of the domain mesh used in the transient electromagnetic FEA is shown in Fig. 8. The domain is split into sub domains where mesh topologies are chosen such that movement of the coil and plunger can be done without comprising the mesh quality. The mesh density are increased in areas around the coil regions to improve the model accuracy.

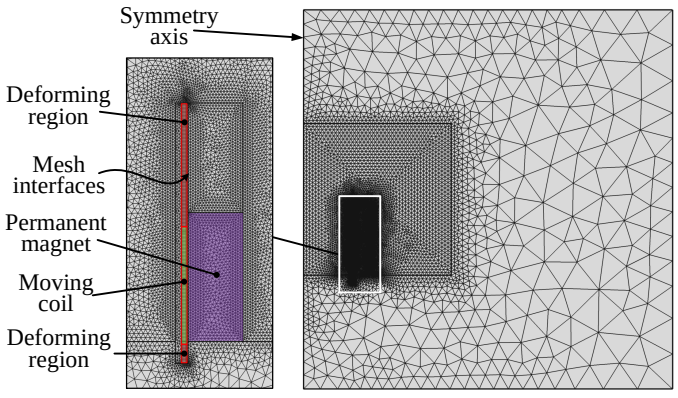

Figure 8. Domain mesh with insulation boundaries, symmetry axis and an increased mesh density near the coil region. The moving/deforming regions are non-conformal and mesh interfaces are used to combine the sub domain regions. Each generated mesh consist of 15-30k elements.

Figure 9 shows an example of a simulation of the LPV's transient response when closing the valve plunger against the seat. The model predicts a valve closing time of approximately 1.2 ms. A voltage step of 550 V is given which builds up the coil current and the actuator force simultaneously. This happens simultaneously due to the initial magnetic field generated by the permanent magnets. The resulting force is initially zero since the actuator force must overcome the opening springs to initiate motion. The fluid force increases significantly as the plunger approaches the valve seat.

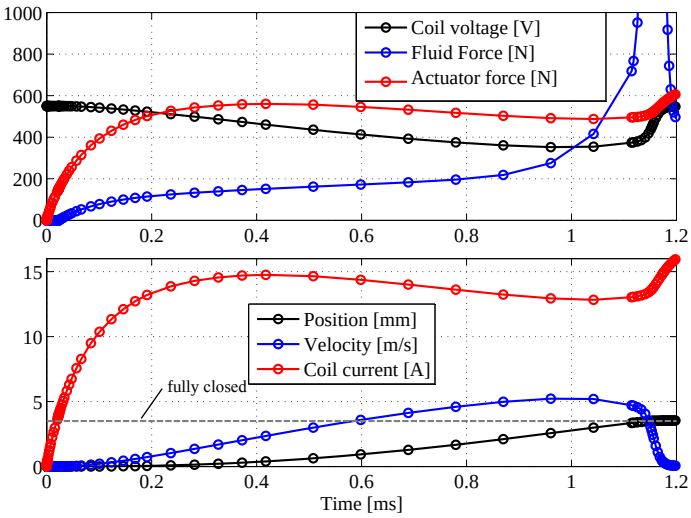

Figure 9. Simulated time dependent response of LPV with a supply voltage of 550 V. The shown coil voltage is the supply voltage with the back-emf subtracted. The valve closing time is predicted to 1.2 ms.

STRUCTURAL FEA OF PLUNGER AND BOBBIN

In the actuator design the coil air gap acts as guide for the bobbin and plunger, hence the clearances must be relatively low. At the same time, the clearances must be sufficiently large to allow for free movement of the bobbin when deforming under pressure. The bobbin is compressed by the pressure because it has a larger surface area on the outside than the inside. To ensure that the air gap contains sufficient free space on both sides of the bobbin and coil at all pressure levels a static structural FEA have been carried out to determine the bobbins maximum deformation under the rated pressure of 400 bar. The FEA is carried out through the software package Ansys 15.0 Workbench.

To accurately predict the deformation of the bobbin (including plunger and coil) the mechanical strength of the coil wound onto the bobbin should be included in the structural FEA. Each turn of the wound copper coil is glued to the bobbin and/or the adjacent coil turns with a fast hardening glue. Since the coil is wound through a manual process, deviations in glue thickness are expected. Thus, predicting the mechanical strength of the

coil is a difficult and comprehensive task. Instead the deformation have been simulated with a solid copper ring attached to the bobbin (with dimensions accordingly the the coil) as a conservative estimate of the coils strength. The bobbin and plunger are designed to be manufactured in a carbon reinforced Poly-Ehter-Ether-Ketone (PEEK) as this composite material exhibits high strength and low density [22]. The static structural FEA revealed a decrease in bobbin diameter of less than 10 μm at 400 bar both with and without the coil winding included in the FEA. Following Eqn. 2 the viscous shearing friction coefficient B only varies vaguely hence the plungers time dependent response is expected to be more or less independent of pressure. Unfortunately, it proved to be difficult to produce an accurate and symmetric prototype specimen using the carbon reinforced PEEK. Therefore, pure PEEK have been used in the prototype as it was easier to process. Without the carbon reinforcement the structural strength of the bobbin and plunger is decreased significantly. Similarly, static FEA have been performed to determine the increase in viscous shearing friction when deforming under pressure. Figure 10 shows deformation along the z-axis in a color plot. The maximum directional deformation correspond to a decrease in diameter of 0.167 mm which according to Eqn. 2 corresponds to an increase in B of approximately 600 % (from 2.4 to 12.5 Ns/m). At the time of maximum velocity the shearing friction equals approximately 70 N hence the transient valve response is expected to be somewhat dependent on the oil pressure that surrounds the plunger and bobbin.

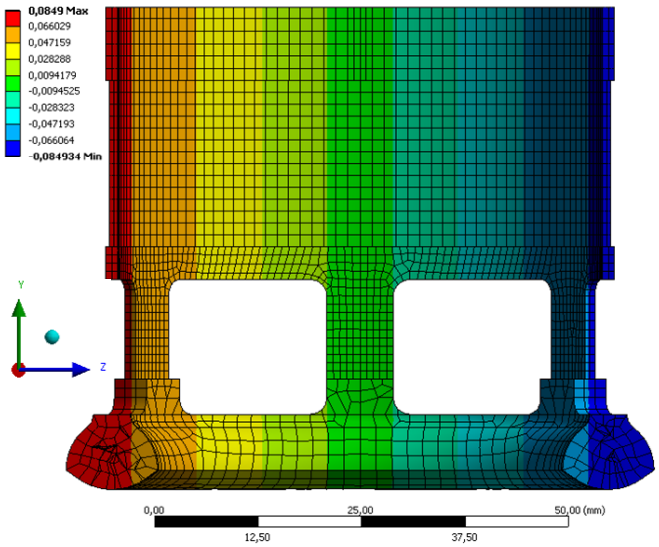

Figure 10. Result of FEA performed on simplified geometry where pure peek is used. The maximum directional deformation corresponds to a decrease in diameter of 0.167 mm. Mesh is hex-dominant with approximately 15k elements.

VALVE PROTOTYPE AND EXPERIMENTAL SETUP

The manufactured valve prototype and the experimental setup is installed in the fluid power laboratory at the Department of Energy Technology at Aalborg University. Figure 11 shows a CAD drawing of the prototype in a sectional view.

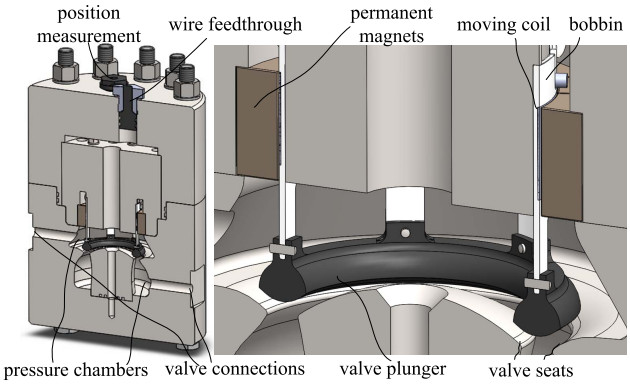

Figure 11. Sectional view of the prototype.

The permanent magnets used in the valve prototype are neodymium shell magnets which have been glued together during assembly. The static magnetic field in the air gap have been experimentally verified (average static field is approximately 1 T) [21]. Also, the current-force ratio have been experimentally verified showing a close to linear relationship between coil current and electromagnetic force (current/force gain is 35 N/A) [21]. The coil has manually been wound onto the bobbin whilst fast hardening glue have been applied. Due to limited experience with the coil wounding process, the prototype coil thickness ($\boldsymbol{b}$ in Fig. 7) ended up exceeding the specified dimensions, even with less coil turns. This implies reduced air gap clearances hence the bobbin experience increased friction. Surprisingly, when moving the plunger in the assembled prototype a static friction force is present. This indicates that the the bobbin/coil is not fully lubricated which influences the transient response. For measurement of the valve plunger position, a rod is connected to the bobbin which is fed through the entire housing. At the far end of the rod, a permanent magnet is attached. A fixed Hall element, generating a voltage output that depends on magnetic flux density, is used to measure the valve plunger position. The prototype has been pressurized using a manual pump connected to a valve connection while the other valve connection is blocked. The valve, including the wire feed through has been pressurized up to 400 bar without leaking. The valve is designed to have springs installed preloaded with a force of 150 N, but during experiments these are omitted. Table 4 gives the actual specifications of the prototype with the design goal values in parentheses. The voltage step is supplied by a Pulse-Width-Modulation (PWM) power

supply board controlled a Field-Programmable-Gate-Array unit. The PWM power supply board is of transiently supplying 20 A at 500 V. The plunger position, the input voltage and the coil current are measured and logged using an oscilloscope.

Table 4. Main specifications of prototype.

Power supply	550V/18.2A	Coil layers	2
Rated flow	600 l/min	Coil resistance	13.7 (26.8) Ω
Rated pressure	350 bar	Coil turns	153 (200)
Pressure drop	$<$ 0.5 bar	Coil height	20 mm
Moving mass	37 g	Wire diameter	0.21 (0.2) mm
Spring preload	150 N	Act. gain	35 N/A
Stroke length	3.5 mm	Plunger diameter	60 mm

EXPERIMENTAL RESULTS AND MODEL VALIDATION

The simulation results of the FEA actuator model and the lumped parameter fluid force model are compared against measurements. Initially, the pressure dependency of the Coulomb friction force is investigated for model accuracy and evaluation of the mechanical design. This is followed by tests of the actuators transient performance during valve closing under various pressures and input voltage levels.

PRESSURE DEPENDENCY

The structural FEA predicts the bobbin to deform when pressurized leading to increased shearing friction. In addition, the air gap clearance in which the bobbin have to move is reduced due to an inaccurate prototype specimen. This leads to a static friction force which indicates that the bobbin and coils shearing areas not are fully lubricated. The constant friction force varies with the pressure, as the bobbin deforms, which influences the transient performance. The static friction force have been determined at various pressures by slowly increasing coil current until movement of the plunger is initiated. Figure 12 shows the relationship between the static friction force and pressure. At large pressures, the static friction force constitutes 15-30 % of the available actuator force at max current. Therefore, a static friction term, as a function of pressure, is included in the simulation model to improve model accuracy. Furthermore, analysis of the transient response revealed that the viscous friction also varied with the pressure as predicted based on the static structural analysis and Eqn. 2. The structural FEA models the deformation as a function of pressure, however due to the inaccuracy of the prototype specimen, the simulation results are can not be used to estimate the shearing layer thickness accurately. As mentioned, the bobbin and coil are not fully lubricated, this implies that the bobbin and or coil is in contact with housing. When pressurized, the bobbin clamps around the inner actuator housing thus the structural FEA results are not applicable since the housing is not included in the model. Instead, the shearing friction have iteratively been tuned at various pressures for the measured and simulated transient response to comply. Further effort should be made to accurately model the friction as a function of pressure but this is disregarded since future prototypes are expected to be more accurately manufactured.

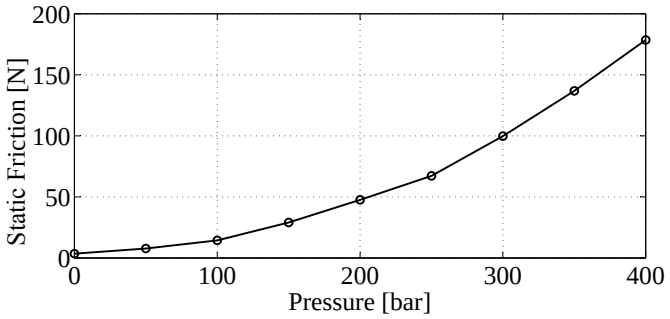

Figure 12. Variation of static friction force due to deformation of bobbin under pressure.

TIME DEPENDENT RESPONSE

The time dependent response is examined with a voltage step given as input at different pressure levels. The voltage step is conducted by applying a fixed voltage level while the valve closes. Sample results are given in Fig. 13 where the measured coil current and plunger position and the corresponding simulations with the pressure being zero and 200 bar are compared. The average voltage given in both experiment and simulation is 270 V. The simulations and the measurements exhibit similar characteristics but some deviations occur. For instance, the measured plunger position is delayed in its response compared to the simulated. When the plunger is rapidly accelerated from standstill, stiction phenomenons may occur which oppose initiation of movement. This have not been included in the fluid force model given in Eqn. 1because initial studies indicates that stiction forces are small. When the plunger is close to fully open an increase in coil current is present both in the measurements and the simulations. This is partly because of a decrease in the generated back-emf as the plunger is slowed down but also because of an increased fluid force. Both the measurements and the simulations shows the plunger slows down before reaching the fully opened position. This indicates that the fluid force model predicts characteristic of the opposing fluid force, but it is not possible to conclude on the model accuracy as mechanical friction phenomenons are dominating the transient response of the valve prototype. The transient electromagnetic FEA appears to be relatively accurate based on the initial current rise which is similar. Table 5 shows the measured and simulated switching time at various voltage level and pressures.

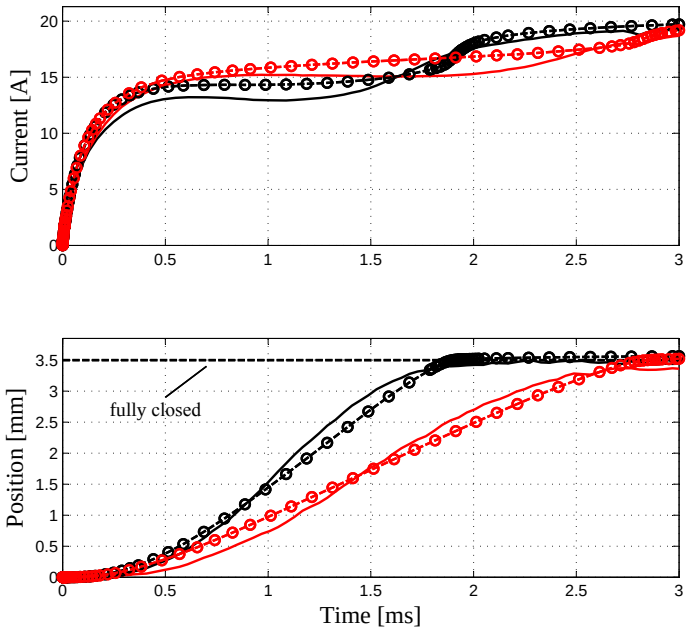

Figure 13. Measured (full line) and simulated (dotted line) transient response for the actuator prototype for a voltage input of 270 at different pressure levels. The black lines are at atmospheric pressure while the red lines are for 200 bar.

Table 5. Measure and simulated switching time at various voltage levels and pressures.

	$T_s(\text{voltage})\|_{1\text{bar}}$			
Coil voltage [V]	90	185	270	380
Shearing friction coeff. [Ns/m]	14.8	14.8	14.8	14.8
Measurements [ms]	4.1	2.6	1.9	1.5
Simulations [ms]	4.2	2.7	1.9	1.5
	$T_s(\text{pressure})\|_{270\text{V}}$			
Pressure [bar]		100	200	300
Shearing friction coeff. B [Ns/m]		18.6	21.2	24.5
Measurements [ms]		2.7	2.1	1.8
Simulations [ms]		2.8	2.2	1.9

CONCLUSION

The time dependent response of a large flow fast switching hydraulic valve prototype has been experimentally tested. The valve prototype features a direct actuator seat valve where a moving coil actuator is used as the force producing element. The prototype design is modelled based on a mathematical framework which partially has been validated through the tests. The valve prototype, including wire feed through to the coil, showed to be leakage free up to a pressure of 400 bar.

FEA simulation of the actuator coupled with the lumped parameter fluid force model proves to be a relatively accurate method to predict the switching time of a fast switching hydraulic valve. Some deviations were seen in position and coil waveform in the transient response which are ascribed mechanical friction and fluid friction phenomenons which are not included in the simulations.

The moving coil actuator design uses the coil air gap as guidance when moving the plunger and bobbin. Using this approach should be done with caution as the bobbin and plunger have been shown through structural FEA to deform when pressurising the valve chambers. During testing of the valve prototype it was found that the time dependent response was strongly dependent on the pressure. This must be considered, especially in the high pressure valve since it experience high pressure levels. This can be avoided by designing the moving coil actuator such that the coil air gap and the bobbin guidance is separated. Furthermore, the air gap clearances are too small in the valve prototype design because of inaccuracies in the manufactured prototype. Therefore, the bobbin and coils shearing areas are not fully lubricated hence a static friction force is present.

Further work is to test the transient performance of the valve when conducting flow and to test the mechanical strength and robustness of the valve by running a large number of cycles.

ACKNOWLEDGEMENT

This work is funded by the Danish Council for Strategic Research via the HyDrive-project (case no. 130500038B). The authors are grateful for the funding.

REFERENCES

[1] Roemer, D., 2014. "Design and optimization of fast switching valves for large scale digital hydraulic motors". PhD thesis.

[2] Roemer, D., Johansen, P., Pedersen, H., and Andersen, T., 2013. "Analysis of valve requirements for high-efficiency digital displacement fluid power motors". In Proceedings of the 8th International Conference on Fluid Power Transmission and Control , ICFP 2013, World Publishing Cooperation, pp. 122–126.

[3] Payne, G., Kiprakis, A., Ehsan, M., Rampen, W., Chick, J., and Wallace, A., 2007. "Efficiency and dynamic performance of digital displacement hydraulic transmission in tidal current energy converters". *Proceedings of the Institution of Mechanical Engineers, Part A: Journal of Power and Energy,* ***221***(2), pp. 207–218.

[4] Ltd, A. I. P., 2013. 7 MW DD Transmission - Progress Report. Wind Power Monthly, November. video available at www.artemisip.com/news-meadia/videos.

[5] Vries, E. D., 2012. Mitsubishi launches 7MW turbine. Wind Power Monthly, January.

[6] Payne, G., Stein, U., Ehsan, M., Caldwell, N. J., and Rampen, W. H., 2005. "Potential of digital displacement hydraulics for wave energy conversion". In In proc. of the 6th European Wave and Tidal Energy Conference.

[7] Rampen, W. H., Almond, J., and Salter, S., 1994. "The digital displacement pump/motor operating cycle: Experimental results demonstrating the fundamental characteristics bath". In International Fluid Power Workshop, Bath.

[8] Roemer, D., Johansen, P., Pedersen, H., and Andersen, T., 2014. "Design method for fast switching seat valves for digital displacement machines". In Proceedings of the 8th FPNI PhD Symposium on Fluid Power, American Society of Mechanical Engineers.

[9] Winkler, S., 2007. "Development of a fast seat type switching valve for big flow rates". In The Tenth Scandinavian International Conference on Fluid Power, SICFP'07, Tampere, Finland, May 21-23, 2007, Vol. 2, pp. 137–146.

[10] Winkler, Plockinger, S., 2010. "A novel piloted fast switching multi poppet valve". *International Journal of Fluid Power,* ***11***(3), 11, pp. 7–14.

[11] Salter, S., and Rampen, W., 1993. Pump control method and poppet valve therefor, Mar. 2. US Patent 5,190,446.

[12] Salter, S., and Rampen, W., 1992. Improved fluid-working machine., July 15. EP Patent App. EP19,900,915,148.

[13] Ltd, A. I. P., 2015. Products - Industrial Hydraulic Pump, April. information available at http://www.artemisip.com/products.

[14] Quilter, J., 2011. Mitsubishi to unveil 7 mw offshore turbine. Wind Power Monthly, November. acessed April 2015 at http://http://www.windpowermonthly.com/.

[15] Stephen, S., Uwe, S., Henry, D., Robert, F., Alasdair, R., and Tom, M., 2013. Method and apparatus for performing maintenance on hydraulic pump, and power generating apparatus of renewable energy type, May 8. CN Patent App. CN 201,180,031,163.

[16] Kameda, T., Uchida, M., Uehara, O., Dodson, H., Robertson, A., and Rampen, W., 2014. Hydraulic pump, method for maintaining same, and wind power generation device, July 23. EP Patent App. EP20,130,809,430.

[17] Tsutsumi, K., Noguchi, T., Korematsu, Y., Shimizu, M., Robertson, A., Stein, U., and Karstens, H., 2012. Hydraulic pump structure for wind turbine generator or tidal current generator and method of mounting hydraulic pump, Nov. 28. CN Patent App. CN 201,080,003,097.

[18] Roemer, D., Johansen, P., Pedersen, H., and Andersen, T., 2013. "Topology selection and analysis of actuator for seat valves suitable for use in digital displacement pumps/motors". In Proceedings of the 2013 IEEE International Conference on Mechatronics and Automation (ICMA), IEEE Press, pp. 418–424.

[19] Roemer, D., Johansen, P., Pedersen, H., and Andersen, T., 2014. "Optimum design of seat region in valves suitable for digital displacement machines". *International Journal of Mechatronics and Automation,* ***4***(2), pp. 116–126.

[20] Furlani, E. P., 2001. *Permanent Magnet and Electromechanical Devices*. Elsevier, Rochester, New York, U.S.A.

[21] Roemer, D., Johansen, P., Bech, M., and Pedersen, H., 2014. "Simulation and experimental testing of an actuator for a fast switching on-off valve suitable to efficient displacement machines". In Proceedings of the 9th JFPS International Symposium on Fluid Power, Japan Fluid Power System Society.

[22] Fujihara, K., Huang, Z.-M., Ramakrishna, S., Satknanantham, K., and Hamada, H., 2003. "Performance study of braided carbon/peek composite compression bone plates". *Biomaterials,* ***24***(15), pp. 2661 – 2667.